Title

Spitzer Spectra of Seyfert Galaxies

Permalink

https://escholarship.org/uc/item/5rq5513s

Journal

STARBURST-AGN CONNECTION, 408

Authors

Spinoglio, Luigi
Tommasin, Silvia
Malkan, Matthew A
et al.

Publication Date

2009

Peer reviewed

Spitzer spectra of Seyfert galaxies

Luigi Spinoglio & Silvia Tommasin

Istituto di Fisica dello Spazio Interplanetario, INAF, Via Fosso del Cavaliere 100, I-00133, Roma, Italy

Matthew A. Malkan & Kevin Hainline

Astronomy Division, University of California, Los Angeles, CA 90095-1547, USA

Abstract. The Spitzer IRS high resolution spectra of about 90 Seyfert galaxies from the 12μm Galaxy Sample are presented and discussed. These represent about 70% of the total complete sample of local Seyfert galaxies. The presence of starburst components in these galaxies can be quantified by powerful mid-IR diagnostics tools (i.e. 11.25μm PAH feature equivalent width and the H_2 emission line intensity) as well as the AGN dominance can be measured by specific fine structure line ratios (e.g. [NeV]/[NeII], [NeV]/[SiII], etc.). The observed line ratios are compared to the results of semianalytical models, which can be used to compute the AGN and starburst contributions to the total luminosity of the galaxies. The results are also discussed in the light of unification and evolution models.

1. Mid-IR spectroscopy with *Spitzer*

We briefly describe here some of the results of the mid-IR spectroscopic survey of Seyfert galaxies belonging to the 12μm Galaxy sample (hereafter 12MGS)(Rush, Malkan & Spinoglio 1993).

The first results of the *Spitzer* spectroscopic survey of the Seyfert galaxies of the 12μm sample (Tommasin et al 2008) show a clear inverse trend between the indicator of *AGN dominance*, the [NeV]14.3μm/[NeII]12.8μm line ratio, and the equivalent width of the 11.25μm PAH feature, which can be considered as an indicator of the *star formation dominance*, as shown in Figure 1a, where the sample objects increaed from 30 (Tommasin et al 2008) to 87 (Tommasin et al 2009). This result confirms an early finding of the ISO-SWS spectrometer (Genzel et al 1998) with a much better statistics. Here the Seyfert galaxies have been reclassified, following the results of spectropolarimetry **(author?)** (Tran 2001, Tran 2003), in type 1's (including the classical Seyfert 1's and the hidden Broad Line Region Seyfert 2's, as discovered through spectropolarimetry) and "pure" type 2's (for which a BLR was not detected). Most of the type 1 objects, including both Seyfert 1s and hidden Broad Line Region Seyfert 2s, are located at high values of the [NeV]14.3μm/[NeII]12.8μm line ratio and very low or absent PAH emission.

Another diagnostic diagram using both spectroscopic and photometric results is shown in Figure 1b: the spectral index between 25 and 60μm $\alpha_{(60\mu m-25\mu m)}$ versus the [NeV]14.3μm/[NeII]12.8μm line ratio. A clear trend shows that when
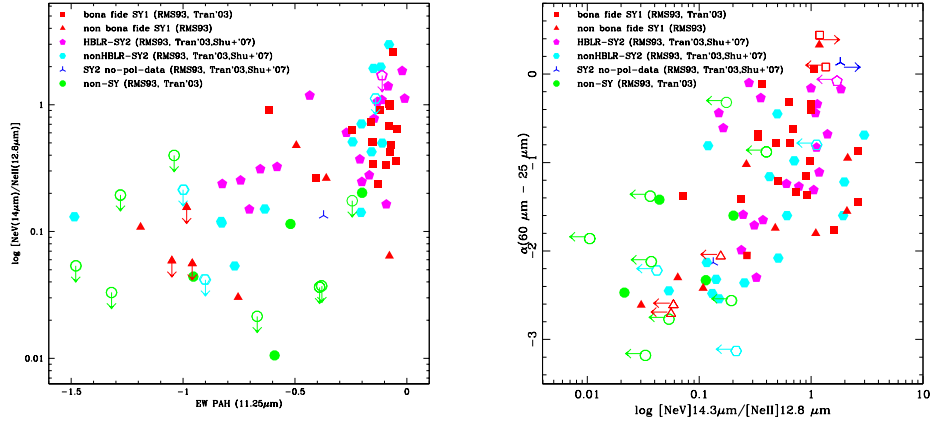
Figure 1.   **a:(left)** [NeV]14.3μm/[NeII]12.8μm line ratio versus the equivalent width of the 11.25μm PAH. **b:(right)** The mid-to-far-IR spectral index $\alpha_{(60\mu m - 25\mu m)}$ versus the [NeV]14.3μm/[NeII]12.8μm line ratio (Tommasin et al 2008; Tommasin et al 2009).

the *AGN dominance* increases, the spectral index flattens. Most of type 1 objects appear to be concentrated in the upper right part of the diagram, at high values of *AGN dominance* and flat mid-to-far-IR slopes.
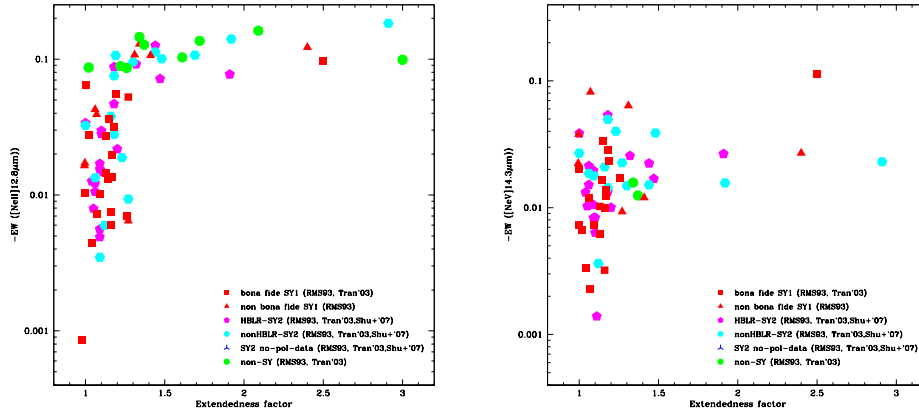

Figure 2.   **a:(left)** [NeII]12.8μm line equivalent width as a function of the source extendedness. **b:(right)** [NeV]14.3μm line EW versus source extendedness (Tommasin et al 2008; Tommasin et al 2009).

The two channels of the Spitzer high-resolution spectrometer: SH 9.6-19.5μm with slit size 4.7$''$ × 11.3$''$ and LH 19-39μm with slit size 11.1$''$ × 22.3 $''$ allow multi-aperture photometry in the overlapping parts (19.0-19.5μm). The ratio of the flux measured in LH to that measured in SH gives the extendedness of the source. We used this measure of the extendedness of the source to estimate the line emitting regions (Tommasin et al 2008). In Figure 2a we plot

the [NeII]12.8μm line equivalent width as a function of the source extendedness. We notice that those sources showing a significant mid-IR extendedness are mostly type 2 objects or non-Seyfert galaxies and have the highest [NeII]12.8μm line equivalent width, with only two exceptions of very nearby Seyfert 1's. An high [NeII]12.8μm line equivalent width is a measure of a strong star formation component. This is not the case for the high excitation lines, originated from the AGN, such as [NeV], for which no apparent trend appears between source extendedness and line EWs , as can be seen in Figure 2b (Tommasin et al 2008).

2. Semianalytical models to estimate AGN and Starburst components

To estimate the percentage of the contribution of AGN and Starburst in the observed emission in a galaxy at 19μm, we computed an analytical model, for each of the observed quantities as a function of R, which is defined as the ratio of the Starburst flux at 19μm to the AGN flux at the same wavelength. R varies from zero - emission totally from the AGN - to infinity - emission totally from the Starburst. The chosen observed quantities are: the extendedness of the source, the equivalent width of PAH at 11.25μm and [NeII] at 12.81μm, the line ratio [NeV]14.32μ/[NeII]12.81μm, the spectral index α at (60-25)μm.

In Fig.3a and 3b the diagrams of [NeV]/[NeII] vs α(60-25)μ m and EW [NeII] vs EW PAH, are shown as examples, where the black curves represent the models. By inverting the models, i.e. solving the analytical expressions with the true values of the observed quantities, we obtained a value of R for each of the five observed quantities of every source. We then computed the mean value of R to estimate the relative percentage of AGN and Starburst emissions.

The sample of sources to which we apply this analysis is reduced because the models depend on the extendedness and the PAH equivalent width, which are not detected (for the PAH) or measurable (for the extendedness) for all the sources(from 86 to 59 objects). We found that the model can disentangle the AGN and the Starburst emission for 16 of 20 Seyfert 1's, 14 of 16 HBLR's, 13 of 14 nonHBLR's, 7 of 9 objects re-classified as not Seyferts. The details of this approach will appear in Tommasin et al. (2009).

3. Analysis of the 12μm sample multi-frequency dataset

The 12MGS has been observed extensively from the radio to the X-rays and we can use the large set of data to search for correlations between different observed quantities. To show an example, we want to relate the X-ray luminosity, measuring the accretion, to the bolometric luminosity, as given by the 12μm luminosity. We plot in Figure 4 the *unabsorbed* 2-10keV luminosity and the 12μm luminosity.

Following the finding of Spinoglio & Malkan (1989) and Spinoglio et al (1995) that the 12μm luminosity is linearly proportional to the *bolometric* luminosity, at a given L$_{bol}$ in Figure 4a a sequence can be identified with decreasing accretion luminosity: from Seyfert 1's $\rightarrow$ HBLR-Seyfert 2's $\rightarrow$ *pure* Seyfert 2's. Although these results are to be considered preliminary, as no statistical method has yet been applied, most Seyfert 1's have:
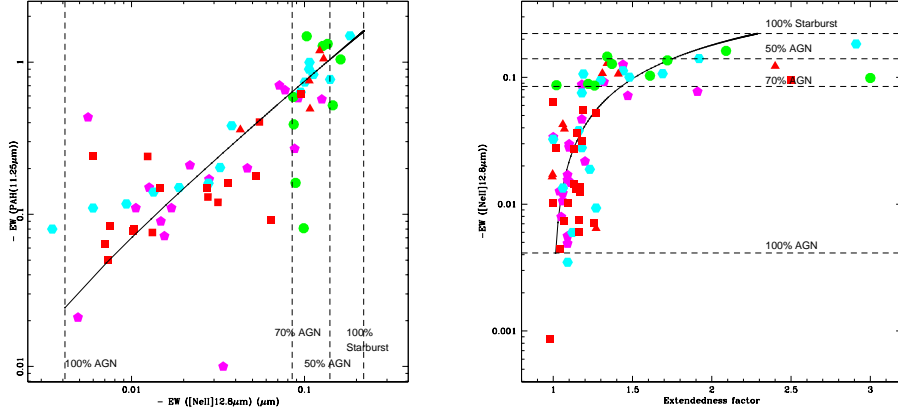
Figure 3.   **a:(left)** The spectral index $\alpha_{(60\mu m-25\mu m)}$ versus the [NeV]14.3μm/[NeII]12.8μm line ratio: the solid line fitting the data is the model and the dashed lines separate the diagram in 3 regions with different AGN contribution, (100% - 70%),(70% - 50%), (50% - 0%). **b:(right)** EW [NeII]12.8μm vs EW PAH 11.25μm: same notation as in Fig.3a.

$$0.1 \times L(12\mu m) < L(2 - 10keV) < L(12\mu m)$$
Most HBLR-Seyfert 2's have:
$$0.01 \times L(12\mu m) < L(2 - 10keV) < 0.1 \times L(12\mu m)$$
Most pure Seyfert 2's and non-Seyfert's have:
$$L(2 - 10keV) < 0.01 \times L(12\mu m)$$

We preminilarily suggest that black hole accretion, as measured by X-rays, is the dominant mechanism determining the observational nature of a galaxy: when accretion is not an important energy source, we have galaxies without Seyfert nuclei, dominated by stellar evolution processes (called here non-Seyfert's), then when accretion increases we have a sequence from the *pure* Seyfert 2's, to the HBLR-Seyfert 2's and finally when accretion dominates the bolometric luminosity, we have the Seyfert 1's.

In an analogous way, we try to correlate the IRAS 60μm luminosity (measuring the integrated star formation activity) and the H$_2$ S(1) line luminosity (typical star formation indicator) in Figure 4b
Most Seyfert 1's and HBLR-Seyfert 2's have:
$$L(H_2) \sim 5 \times 10^{-4} \times L(60\mu m)$$
Most pure Seyfert 2's and non-Seyfert have:
$$L(H_2) \sim 10^{-4} \times L(60\mu m)$$
If we make least squares fits to the two extreme populations of Seyfert type 1's and non-Seyfert galaxies, we obtain a sequence of two almost parallel lines of the form $Log(L(60\mu m)) = a \times log(L(H_2)) + b$ from the bottom to the top:

- for Seyfert 1's: a=0.905, b=7.325, with a regression coefficient of R=0.928;

- for non-Seyfert's: a=1.030, b=2.797, with R=0.925.

There are two interpretations of this behavior: either the more active galaxies (type 1's) have enhanced H$_2$ emission (Rigopoulou et al 2002), or at a given
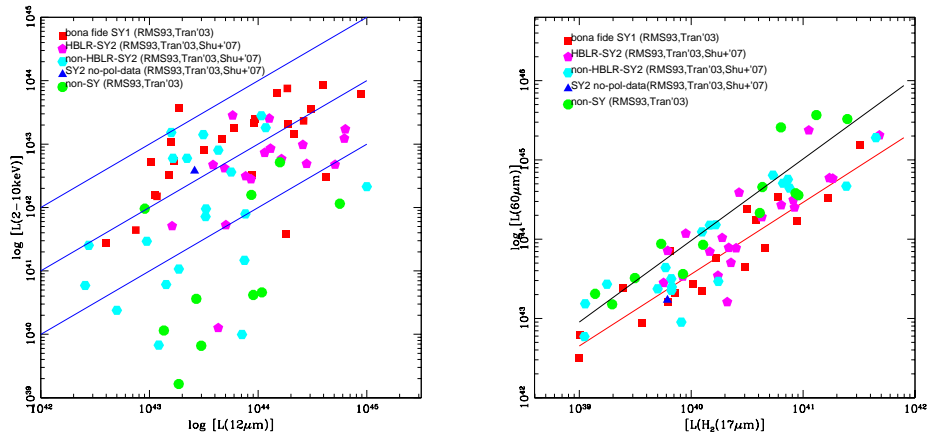
Figure 4.   **a:(left)** Corrected (unabsorbed) X-ray (2-10 keV) luminosity as a function of the $12\mu m$ luminosity. The three lines from the top to the bottom indicate the loci of L(2-10keV) = L($12\mu m$) (*upper*); L(2-10keV) = 0.1 $\times$ L($12\mu m$) (*middle*); and L(2-10keV) = 0.01 $\times$ L($12\mu m$) (*lower*), which are used in the text to roughly separate the different objects. **b:(right)** Total $60\mu m$ luminosity as a function of the H_2 $17\mu m$ line luminosity. The two lines from the top to the bottom are least squares fits of the non-Seyfert galaxies and of the Seyfert 1's, respectively (see the text)

H_2 luminosity, type 2's (and non-Sy) have $L(60\mu m)$ 5 times higher than type 1's, because of an enhanced star formation process.

References

Genzel, R. et al, 1998, ApJ, 498, 579

Rigopoulou, D., Kunze, D., Lutz, D., Genzel, R., & Moorwood, A.F.M. 2002, A&A, 389, 374

Rush, B., Malkan, M.A., & Spinoglio, L. 1993, ApJS, 89, 1 (RMS).

Spinoglio, L. & Malkan, M.A. 1989, ApJ, 342, 83

Spinoglio, L., Malkan, M.A., Rush, B., Carrasco, L., Recillas-Cruz, E. 1995, ApJ, 453, 616

Tommasin, S., Spinoglio, L., Malkan, M.A., Smith, H., Gonzalez-Alfonso, E. & Charmandaris, V. 2008, ApJ, 676, 836.

Tommasin, S., Spinoglio, L., Malkan, M.A., Smith, H. 2009, in preparation

Tran, H.D., 2001, ApJ, 554, L19

Tran, H.D., 2003, ApJ, 583, 632